

---

# Is Homophily a Necessity for Graph Neural Networks?

---

**Yao Ma**

New Jersey Institute of Technology  
 majunyao@gmail.com

**Xiaorui Liu**

Michigan State University  
 xiaorui@msu.edu

**Neil Shah**

Snap Inc.  
 nshah@snap.com

**Jiliang Tang**

Michigan State University  
 tangjili@msu.edu

## Abstract

Graph neural networks (GNNs) have shown great prowess in learning representations suitable for numerous graph-based machine learning tasks. When applied to semi-supervised node classification, GNNs are widely believed to work well due to the homophily assumption (“like attracts like”), and fail to generalize to heterophilous graphs where dissimilar nodes connect. Recent works design new architectures to overcome such heterophily-related limitations, citing poor baseline performance and new architecture improvements on a few heterophilous graph benchmark datasets as evidence for this notion. In our experiments, we empirically find that standard graph convolutional networks (GCNs) can actually achieve better performance than such carefully designed methods on some commonly used heterophilous graphs. This motivates us to reconsider whether homophily is truly necessary for good GNN performance. We find that this claim is not quite true, and in fact, GCNs can achieve strong performance on heterophilous graphs under certain conditions. Our work carefully characterizes these conditions, and provides supporting theoretical understanding and empirical observations. Finally, we examine existing heterophilous graphs benchmarks and reconcile how the GCN (under)performs on them based on this understanding.

## 1 Introduction

Graph neural networks (GNNs) are a prominent approach for learning representations for graph structured data. Thanks to their great capacity in jointly leveraging attribute and graph structure information, they have been widely adopted to promote improvements for numerous graph-related learning tasks [18, 13, 37, 8, 43], especially centered around node representation learning and semi-supervised node classification (SSNC). GNNs learn node representations by a recursive neighborhood aggregation process, where each node aggregates and transforms features from its neighbors. The node representations can then be utilized for downstream node classification or regression tasks. Due to this neighborhood aggregation mechanism, existing literature posits that strong *homophily* of the underlying graph is a necessity for GNNs to achieve good performance on SSNC [1, 41, 40, 4, 22, 12, 14, 35]. In general, homophily describes the phenomenon that nodes tend to connect with “similar” or “alike” others. Homophily is observed in a wide range of real-world graphs including friendship networks [23], political networks [10, 25], citation networks [5] and more. Under the homophily assumption, through the aggregation process, a node’s representation is “smoothed” via its neighbors’ representations, since each node is able to receive additional information from neighboring nodes, which are likely to share the same label. Several recent works [41, 40] claim that GNNs are implicitly (or explicitly) designed with homophily in mind, are not suitable for graphs exhibiting *heterophily*, where connected nodes are prone to have different properties or labels, e.g. dating

networks or molecular networks [41]. To address this limitation, these works accordingly design and modify neural architectures and demonstrate outperformance over other GNN models on several heterophilous graphs. However, we empirically find that the standard graph convolutional network (GCN) [18], a fundamental, representative GNN model which we focus on in this work is actually able to outperform these heterophily-specific models on several heterophilous graphs after careful hyperparameter tuning. This motivates us to reconsider the popular notion in literature that GNNs exhibit a homophilous inductive bias, and more specifically that strong homophily is crucial to strong GNN performance. Counter to this idea, we find that the standard GCN model has the potential to work well for heterophilous graphs under suitable conditions. We demonstrate simple intuition with the following toy example:

Consider the perfectly heterophilous graph (all inter-class edges) shown in Figure 1, where the color indicates the node label. Blue-labeled and orange-labeled nodes are associated with the scalar feature 0 and 1, respectively. If we consider a single-layer GCN by performing an averaging feature aggregation over all neighboring nodes (without self-connection), it is clear that all blue nodes will have a representation of 1, while the orange nodes will have that of 0. Additional layers/aggregations will continue to alternate the features between the two types of nodes. Regardless of the number of layers, the two classes can still be perfectly separated. In this toy example, each blue (orange) node only connects orange (blue) nodes, and all blue (orange) nodes share similar neighborhood patterns in terms of their neighbors' label/feature distributions. Naturally, real graphs are rather more complicated.

In this work, we elucidate this intuition and extend it to a more general case: put simply, given a (homophilous or heterophilous) graph, GCN has the potential to achieve good performance if nodes with the same label share similar neighborhood patterns. We theoretically support this argument by investigating the learned node embeddings from the GCN model. We further show how GCN performance is only *loosely* linked to homophily or heterophily in the underlying graph, and demonstrate how different notions of heterophily can yield better or worse discriminative performance. Overall, our work makes the following key contributions.

**Our contributions.** (1) We reveal that strong homophily is not a necessary assumption for GCN model. The GCN model can perform well over heterophilous graphs under certain conditions. (2) We carefully characterize these conditions and provide theoretical understanding on how GCNs can achieve good SSNC performance under these conditions by investigating their embedding learning process. (3) We carefully investigate commonly used homophilous and heterophilous benchmarks and reason about GCN's performs on them utilizing our theoretical understanding.

## 2 Preliminaries

Let  $\mathcal{G} = \{\mathcal{V}, \mathcal{E}\}$  denote a graph, where  $\mathcal{V}$  and  $\mathcal{E}$  are the sets of nodes and edges, respectively. The graph connection information can also be represented as an adjacency matrix  $\mathbf{A} \in \{0, 1\}^{|\mathcal{V}| \times |\mathcal{V}|}$ , where  $|\mathcal{V}|$  is the number of nodes in the graph. The  $i, j$ -th element of the adjacency matrix  $\mathbf{A}[i, j]$  is equal to 1 if and only if nodes  $i$  and  $j$  are adjacent to each other, otherwise  $\mathbf{A}[i, j] = 0$ . Each node  $i$  is associated with a  $l$ -dimensional vector of node features  $\mathbf{x}_i \in \mathbb{R}^l$ ; the features for all nodes can be summarized as a matrix  $\mathbf{X} \in \mathbb{R}^{|\mathcal{V}| \times l}$ . Furthermore, each node  $i$  is associated with a label  $y_i \in \mathcal{C}$ , where  $\mathcal{C}$  denotes the set of labels. We also denote the set of nodes with a given label  $c \in \mathcal{C}$  as  $\mathcal{V}_c$ . We assume that labels are only given for a subset of nodes  $\mathcal{V}_{label} \subset \mathcal{V}$ . The goal of semi-supervised node classification (SSNC) is to learn a mapping  $f : \mathcal{V} \rightarrow \mathcal{C}$  utilizing the graph  $\mathcal{G}$ , the node features  $\mathbf{X}$  and the labels for nodes in  $\mathcal{V}_{label}$ .

### 2.1 Homophily in Graphs

In this work, we focus on investigating performance in the context of graph homophily and heterophily properties. Homophily in graphs is typically defined based on similarity between connected node pairs, where two nodes are considered similar if they share the same node label. The homophily ratio is defined based on this intuition.

**Definition 1** (Homophily). *Given a graph  $\mathcal{G} = \{\mathcal{V}, \mathcal{E}\}$  and node label vector  $y$ , the edge homophily ratio is defined as the fraction of edges that connect nodes with the same labels. Formally, we have:*

$$h(\mathcal{G}, \{y_i; i \in \mathcal{V}\}) = \frac{\sum_{(j,k) \in \mathcal{E}} \mathbb{1}(y_j = y_k)}{|\mathcal{E}|}, \quad (1)$$

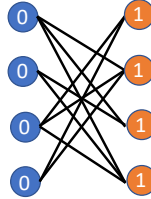


Figure 1: A perfectly heterophilous graph on which GCN achieves perfect class separation.

where  $|\mathcal{E}|$  is the number of edges in the graph and  $\mathbb{1}(\cdot)$  is the indicator function.

A graph is typically considered to be highly homophilous when  $h(\cdot)$  is large (typically,  $0.5 \leq h(\cdot) \leq 1$ ), given suitable label context. In such case, edges predominantly connect nodes with the same labels. On the other hand, a graph with a low edge homophily ratio is considered to be heterophilous. In future discourse, we write  $h(\cdot)$  as  $h$  when discussing given a fixed graph and label context. Note that homophily is a distinct property from heterogeneity; the former refers to class labels of connected nodes, while the latter refers to their types.

## 2.2 Graph Neural Networks

Graph neural networks learn node representations by aggregating and transforming information over the graph structure. There are different designs and architectures for the aggregation and transformation process, which leads to different graph neural network models [29, 18, 13, 34, 11, 39].

One of the most popular and widely adopted GNN models is the graph convolutional network (GCN). The  $k$ -th step of the GCN model takes the following form:  $\mathbf{H}^{(k)} = \sigma(\hat{\mathbf{A}}\mathbf{H}^{(k-1)}\mathbf{W}^{(k)})$ , where  $\sigma(\cdot)$  is some non-linear activation function,  $\mathbf{W}^{(k)} \in \mathbb{R}^{l \times l}$  is a parameter matrix to transform the features, and  $\hat{\mathbf{A}}$  is a normalized adjacency matrix to perform the aggregation. Typically, we use associated node features as the input for the GCN model, i.e.,  $\mathbf{H}^{(0)} = \mathbf{X}$ . Different variants of the normalization matrix can be adopted including the row-normalized adjacency matrix and symmetric adjacency matrix listed as follows:

$$\text{Row Normalized Adjacency Matrix: } \hat{\mathbf{A}} = \mathbf{D}^{-1}(\mathbf{A} + \mathbf{I}) \quad (2)$$

$$\text{Symmetric Adjacency Matrix: } \hat{\mathbf{A}} = \mathbf{D}^{-\frac{1}{2}}(\mathbf{A} + \mathbf{I})\mathbf{D}^{-\frac{1}{2}} \quad (3)$$

where  $\mathbf{D}$  is a diagonal matrix and  $\mathbf{D}[i, i] = \text{deg}(i) + 1$  with  $\text{deg}(i)$  denoting the degree of node  $i$ . The matrix  $\mathbf{I} \in \{0, 1\}^{|\mathcal{V}| \times |\mathcal{V}|}$  is an identity matrix. Hence, adding  $\mathbf{I}$  to the adjacency matrix  $\mathbf{A}$  can be regarded as adding self-connections for nodes.

## 3 Graph Convolutional Networks under Heterophily

Considerable prior literature posits that graph neural networks (such as GCN) work by assuming and exploiting homophily assumptions in the underlying graph [22, 12, 35]. To this end, researchers have determined that such models are considered to be ill-suited for heterophilous graphs, where the homophily ratio is low [41, 40, 4]. To deal with this limitation, researchers proposed several methods including H2GNN [41], CPGNN [40] and GPRGNN [4], which are explicitly designed to handle heterophilous graphs via architectural choices (e.g. adding skip-connections, carefully choosing aggregators, etc.) To demonstrate their assumptions, these works cited the poor SSNC performance of GCN on several heterophilous graphs, and to demonstrate their proposed solutions, they cited their design’s relative outperformance of GCN in these tasks.

In this section, we revisit the claim that GCNs have fundamental homophily assumptions and are not suited for heterophilous graphs. To this end, we first observe empirically that the GCN model achieves fairly good performance on some of the commonly used heterophilous graphs; specifically, we present SSNC performance on two commonly used heterophilous graph datasets, Chameleon and Squirrel in Table 1 (see Appendix D for further details about the datasets and models). Both Chameleon and Squirrel are highly heterophilous ( $h \approx 0.2$ ). We find that with some hyperparameter tuning, GCN can *outperform alternative methods uniquely designed to operate on heterophilous graphs* by a sizeable margin.

This observation suggests that GCN does not always “underperform” on heterophilous graphs, and it leads us to reconsider the prevalent assumption in literature. Hence, we next examine how GCNs learn representations, and how this information is used in downstream SSNC tasks, homophily and heterophily assumptions aside.

Table 1: SSNC accuracy on two heterophilous datasets: standard GCN outperforms all heterophily-specific models on these graphs.

Method	Chameleon ( $h = 0.23$ )	Squirrel ( $h = 0.22$ )
GCN	<b>67.96</b> $\pm$ 1.82	<b>54.47</b> $\pm$ 1.17
H2GCN-1	57.11 $\pm$ 1.58	36.42 $\pm$ 1.89
H2GCN-2	59.39 $\pm$ 1.98	37.90 $\pm$ 2.02
CPGNN-MLP	54.53 $\pm$ 2.37	29.13 $\pm$ 1.57
CPGNN-Cheby	65.17 $\pm$ 3.17	29.25 $\pm$ 4.17
GPRGNN	66.31 $\pm$ 2.05	50.56 $\pm$ 1.51

### 3.1 When does GCN learn *similar* embeddings?

GCNs have been shown to be able to capture the local graph topological and structural information [36, 24]. Specifically, the aggregation step in the GCN model is able to capture and discriminate neighborhood distribution information (more precisely, the mean of the neighborhood features) [36]. Let us consider the two nodes  $a$  and  $b$  shown in Figure 2, where we use color to indicate the label of each node. If we further assume that all nodes share the same label are associated with exactly the same features, then clearly, after 1-step aggregation, the GCN model with the row-normalized adjacency matrix (see Eq. (2); ignoring the self-connection here) will output exactly the same embedding for nodes  $a$  and  $b$  (the average features of “orange”, “yellow” and “green” node). Accordingly, Xu et al. [36] reasons that the GCN model lacks expressiveness since it cannot differentiate nodes  $a$  and node  $b$  in the embedding space, because although they share the same neighborhood *distribution*, they differ concretely in neighborhood *structure* (here, w.r.t. count). However, in this example SSNC task, mapping nodes  $a$  and  $b$  to the same location in the embedding space is not an adverse effect, but explicitly desirable, since they share the same label and we are not concerned with telling them apart. Intuitively, if all nodes with the same label are mapped to the same embedding and embeddings for different labels are distinct, then, nodes are perfectly separable in the embedding space and thus can be effortlessly classified (one instance in which expressive power and task performance do not coincide). One instance in which such separability arises is in the case of the “ideal graph” as mentioned in Zhao et al. [38], which considers a perfectly homophilous graph of  $|\mathcal{C}|$  (fully) connected components, where all nodes in a component share the same label.

Of course, in reality, such idealized graphs which meet these precise assumptions are rare to nonexistent. Thus, to consider a more practical scenario, we assume that both features and neighborhood patterns for nodes with a certain label are sampled from some fixed distributions. Under these conditions, nodes with the same label may not be mapped to exactly the same embedding. Instead, we aim to characterize how close the learned embeddings of same-label nodes are. Intuitively, if the learned embeddings for nodes with the same label are very close, we expect SSNC performance to be good (given that embeddings of nodes of other classes are far), as class separability is high (low intra-class variance and high inter-class variance) [9]. We prove that, for graphs meeting suitable conditions (features and neighborhood pattern for nodes with a certain label are sampled from some fixed distributions), the distance between the embeddings learned by a single GCN layer of any node pair that shares the same label is bounded by a small quantity with high probability. We elaborate below.

**Assumptions on Graphs.** We consider a graph  $\mathcal{G}$ , where each node  $i$  has features  $\mathbf{x}_i \in \mathbb{R}^l$  and label  $y_i$ . We assume that (1)  $\mathcal{G}$  is  $d$ -regular; (2) The features of node  $i$  are sampled from feature distribution  $\mathcal{F}_{y_i}$ , i.e.,  $\mathbf{x}_i \sim \mathcal{F}_{y_i}$ , with  $\mu(\mathcal{F}_{y_i})$  denoting its mean; (3) Dimensions of  $\mathbf{x}_i$  are independent to each other; (4) The features in  $\mathbf{X}$  are bounded by a positive scalar  $B$ , i.e.,  $\max_{i,j} |\mathbf{X}[i,j]| \leq B$ ; (5) For node  $i$ , its neighbor’s labels are independently sampled from neighbor distribution  $\mathcal{D}_{y_i}$ . The sampling is repeated for  $d$  times to sample the labels for  $d$  neighbors.

We denote a graph following these assumptions (1)-(5) as  $\mathcal{G} = \{\mathcal{V}, \mathcal{E}, \{\mathcal{F}_c, c \in \mathcal{C}\}, \{\mathcal{D}_c, c \in \mathcal{C}\}, d\}$ . Note that we use the subscripts in  $\mathcal{F}_{y_i}$  and  $\mathcal{D}_{y_i}$  to indicate that these two distributions are shared by all nodes with the same label as node  $i$ . For regular graphs, the two kinds of normalized adjacency matrices we introduced in Section 2.2 lead to the same GCN model. Specifically, for a single layer GCN model, the process can be written in the following form for node  $i$ :

$$\mathbf{h}_i = \sum_{j \in \{i\} \cup \mathcal{N}(i)} \frac{1}{d+1} \mathbf{W} \mathbf{x}_j, \quad (4)$$

where  $\mathbf{W} \in \mathbb{R}^{l \times l}$  is the parameter matrix and  $\mathbf{x}_j$  is the input features for node  $j$ .  $\mathbf{h}_j$  is the pre-activation output from the GCN model, and an element-wise non-linear activation function can be applied to  $\mathbf{h}_i$  to obtain the final output.

**Theorem 1.** Consider a graph  $\mathcal{G} = \{\mathcal{V}, \mathcal{E}, \{\mathcal{F}_c, c \in \mathcal{C}\}, \{\mathcal{D}_c, c \in \mathcal{C}\}, d\}$ , which follows Assumptions (1)-(5). For any node  $i \in \mathcal{V}$ , the expectation of the pre-activation output of a single-layer GCN model from Eq (4) is given by

$$\mathbb{E}[\mathbf{h}_i] = \mathbf{W} \left( \frac{1}{d+1} \mu(\mathcal{F}_{y_i}) + \frac{d}{d+1} \mathbb{E}_{c \sim \mathcal{D}_{y_i}, \mathbf{x} \sim \mathcal{F}_c} [\mathbf{x}] \right). \quad (5)$$



Figure 2: Two nodes share the same neighborhood distribution; GCN learns equivalent embeddings for  $a$  and  $b$ .

and for any  $t > 0$ , the probability that the distance between the observation  $\mathbf{h}_i$  and its expectation is larger than  $t$  is bounded by

$$\mathbb{P}(\|\mathbf{h}_i - \mathbb{E}[\mathbf{h}_i]\|_2 \geq t) \leq 2 \cdot l \cdot \exp\left(-\frac{(d+1)t^2}{2\rho^2(\mathbf{W})B^2l}\right), \quad (6)$$

where  $l$  is the feature dimensionality and  $\rho(\mathbf{W})$  denotes the largest singular value of  $\mathbf{W}$

*Proof.* The detailed proof can be found in Appendix A.  $\square$

**Theorem 2.** Consider a graph  $\mathcal{G} = \{\mathcal{V}, \mathcal{E}, \{\mathcal{F}_c, c \in \mathcal{C}\}, \{\mathcal{D}_c, c \in \mathcal{C}\}, d\}$ , which follows Assumptions (1)-(5). For any two nodes  $i, j \in \mathcal{V}$  that share the same label, i.e.,  $y_i = y_j$ , the probability that the distance between their output pre-activation embeddings (from Eq. (4)) is larger than  $t$  ( $t > 0$ ) is bounded by

$$\mathbb{P}(\|\mathbf{h}_i - \mathbf{h}_j\|_2 \geq t) \leq 4 \cdot l \cdot \exp\left(-\frac{(d+1)t^2}{8\rho^2(\mathbf{W})B^2l}\right) \quad (7)$$

*Proof.* The detailed proof can be found in Appendix B.  $\square$

**Remark 1.** Theorem 2 can be naturally extended to include non-linear activation functions. Specifically, many commonly used activation functions  $\sigma(\cdot)$  (e.g. ReLU and sigmoid) are 1-Lipschitz continuous [28], i.e.,  $|\sigma(x) - \sigma(y)| \leq |x - y|$ . Hence, we have  $\mathbb{P}(\|\sigma(\mathbf{h}_i) - \sigma(\mathbf{h}_j)\|_2 \geq t) \leq \mathbb{P}(\|\mathbf{h}_i - \mathbf{h}_j\|_2 \geq t)$ .

Theorem 1 demonstrates two key ideas. First, in expectation, all nodes with the same label have the same embedding (Eq. (5)). Second, the distance between the output embedding of a node and its expectation is small with high probability. Building upon Theorem 1, Theorem 2 further demonstrates that two nodes with the same label are thus close to each other with high probability, anchored by their shared expected value. With Remark 1, we further have that the post-activation outputs (e.g. final embeddings from a complete GCN layer with transformation, aggregation and nonlinearity) are also likewise bounded given common, suitable choices. Together, these results show that the GCN model is able to map nodes with the same label close to each other in the embedding space under given assumptions, facilitating the SSNC task earlier discussed. Based on these understandings, we have the following key (informal) observations.

**Observation 1** (GCN under Homophily). *In homophilous graphs, the neighborhood distribution of nodes with the same label (w.l.o.g.  $c$ ) can be approximately regarded as a highly skewed discrete  $\mathcal{D}_c$ , with most of the mass concentrated on the category  $c$ . Thus, different labels clearly have distinct distributions. Hence, the GCN model typically excels in SSNC on such graphs.*

**Observation 2** (GCN under Heterophily). *In heterophilous graphs, if the neighborhood distribution of nodes with the same label (w.l.o.g.  $c$ ) is (approximately) sampled from a fixed distribution  $\mathcal{D}_c$ , and different labels have distinguishable distributions, then the GCN model can excel in the SSNC task.*

Note that the second observation follows from considering a “worst-case” scenario where  $\mathcal{D}_c = \mathcal{D}_{c'}$  for two distinct classes  $c, c'$ , implying that they would be frequently misclassified. Notably, our findings illustrate that disruptions of certain conditions inhibit GCN performance on heterophilous graphs, but heterophily is *neither a sufficient nor necessary condition for poor GCN performance*. Section 3.2 shows experiments bolstering this argument. We note that these “idealized” conditions for GCN SSNC performance we discuss offer a more general perspective than those in prior literature; [38] only discusses perfectly homophilous ( $h = 1$ ) graphs as ideal for SSNC, and several works [12, 35] aim to learn graph structure over independent samples for downstream graph learning tasks using the same perspective. Our findings show that under suitable conditions, heterophilous graphs can also be ideal in terms of effortless node classification. We note that although our derivations are for GCN, a similar line of analysis can be used for more general message-passing neural networks.

### 3.2 How does classification performance change over the homophily-heterophily spectrum?

We next evaluate how downstream performance changes as we make a homophilous graph more and more heterophilous. Prima facie wisdom from prior literature would indicate that performance degrades markedly as heterophily increases, when other factors (e.g. labels, features) are kept fixed.

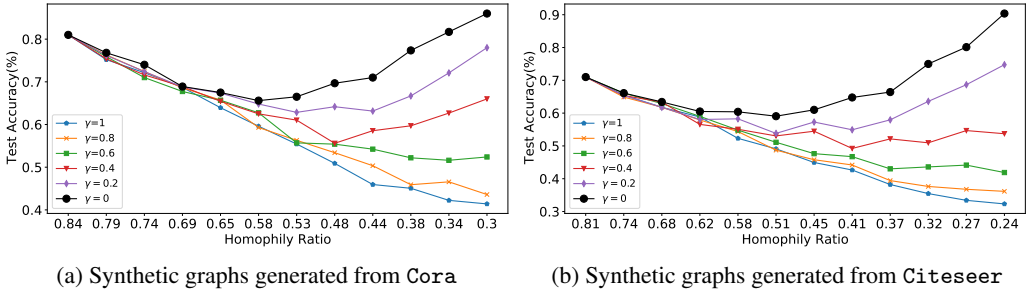


Figure 3: SSNC accuracy of GCN on synthetic graphs with various homophily ratios, generated by adding heterophilous edges according to pre-defined target distributions on Cora (a) and Citeseer (b): performance first decreases, then increases, forming a V-shape (see the black lines).

We next conduct experiments to substantiate our claims in Observations 1 and 2. Specifically, we consider two settings: (1) evaluating classification performance in heterophilous graphs under optimistic assumptions, where different labels have distinct distributions, and (2) evaluating classification performance under more pessimistic cases, where different labels’ distributions are muddled.

### 3.2.1 Targeted Heterophilous Edge Addition

We start with common, real-world benchmark graphs, and modify their topology by adding synthetic, cross-label edges that connect nodes with different labels. Note that we only add cross-label edges to ensure that as more edges are added, the graphs become more and more heterophilous. Following our discussion in Observation 2, we try to construct synthetic graphs that have similar neighborhood distributions for nodes with the same label. Specifically, given a real-world graph  $\mathcal{G}$ , we first define a discrete neighborhood target distribution  $\mathcal{D}_c$  for each label  $c \in \mathcal{C}$ , as per Assumption 5 in Section 3.1. We then follow these target distributions to add cross-label edges. The process of generating new graphs by adding edges to  $\mathcal{G}$  is shown in Algorithm 1. As shown in Algorithm 1, we add a total  $K$  edges to the given graph  $\mathcal{G}$ : to add each edge, we first uniformly sample a node  $i$  from  $\mathcal{V}$  with label  $y_i$ , then we sample a label  $c$  from  $\mathcal{C}$  according to  $\mathcal{D}_{y_i}$ , and finally, we uniformly sample a node  $j$  from  $\mathcal{V}_c$  and add the edge  $(i, j)$  to the graph. In the limit (as  $K \rightarrow \infty$ ), the neighborhood distributions in the generated graph converge to  $\mathcal{D}_{y_i}$  regardless of initial topology, and homophily decreases ( $h \rightarrow 0$ ). We generate synthetic graphs based on several real-world graphs. We present the results based on Cora and Citeseer [30]. The results for other datasets can be found in Appendix C.

Both Cora and Citeseer exhibit strong homophily. The Cora graph consists of 2,708 nodes and 5,278 edges and it has 7 labels. The Citeseer graph has 6 labels and consists of 3,327 nodes and 4,676 edges. For both datasets, we fix  $\mathcal{D}_c$  for all labels. Although many suitable  $\mathcal{D}_c$  could be specified in line with Observation 2, we fix one set for illustration and brevity. For Cora, we specify  $\mathcal{D}_0$  as **Categorical**( $[0, 1/2, 0, 0, 0, 0, 1/2]$ ), in which, the  $(c+1)$ -th element corresponds to the probability mass for sampling a node with label  $c$  as a neighbor; all  $\mathcal{D}_c$  are distinct. For both datasets, we vary  $K$  over 11 values and thus generate 11 graphs. Notably, as  $K$  increases, the homophily  $h$  decreases. More detailed information about the  $\{\mathcal{D}_c, c \in \mathcal{C}\}$  and  $K$  for both datasets is included in Appendix C.

Figure 3(a-b) show SSNC results (accuracy) on graphs generated based on Cora and Citeseer, respectively. The black line in both figures shows results for the presented setting (we introduce  $\gamma$  in the following subsection). Without loss of generality, we use Cora (a) to discuss our findings, since observations are similar over these datasets. Each point on the black line in Figure 3(a) represents the performance of GCN model on a certain generated graph and the corresponding value in  $x$ -axis denotes the homophily ratio of this graph. The point with homophily ratio  $h = 0.85$  denotes the original Cora graph, i.e.,  $K = 0$ . We observe that as  $K$  increases,  $h$  decreases, and while the classification performance first decreases, it *eventually begins to increase*, showing a V-shape pattern. For instance, when  $h = 0.3$  (a rather heterophilous graph), the GCN model achieves an impressive

---

**Algorithm 1:** Heterophilous Edge Addition

---

```

input :  $\mathcal{G} = \{\mathcal{V}, \mathcal{E}\}, K, \{\mathcal{D}_c\}_{c=0}^{|\mathcal{C}|-1}$ 
        and  $\{\mathcal{V}_c\}_{c=0}^{|\mathcal{C}|-1}$ 
output :  $\mathcal{G}' = \{\mathcal{V}, \mathcal{E}'\}$ 
Initialize  $\mathcal{G}' = \{\mathcal{V}, \mathcal{E}\}, k = 1$  ;
while  $1 \leq k \leq K$  do
    Sample node  $i \sim \text{Uniform}(\mathcal{V})$ ;
    Obtain the label,  $y_i$  of node  $i$ ;
    Sample a label  $c \sim \mathcal{D}_{y_i}$ ;
    Sample node  $j \sim \text{Uniform}(\mathcal{V}_c)$ ;
    Update edge set  $\mathcal{E}' = \mathcal{E}' \cup \{(i, j)\}$ ;
     $k \leftarrow k + 1$ ;
return  $\mathcal{G}' = \{\mathcal{V}, \mathcal{E}'\}$ 

```

---

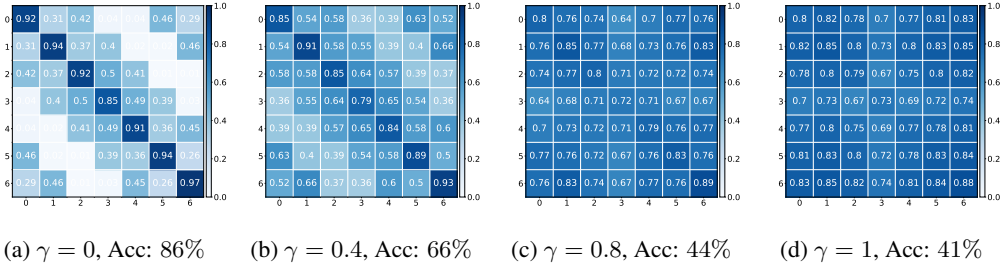


Figure 4: Cross-class neighborhood similarity on synthetic graphs generated from Cora; all graphs have  $h = 0.3$ , but with varying neighborhood distributions as per the noise parameter  $\gamma$ : as  $\gamma$  increases, the intra-class similarity and the inter-class similarity become closer to each other, indicating that the distributions for different classes become more indistinguishable.

86% accuracy, even higher than that achieved on the original Cora graph. We note that performance continues to increase as  $K$  increases further to the right (we censor due to space limitations). This clearly demonstrates that the GCN model can work well on heterophilous graphs under certain conditions. Intuitively, the  $V$ -shape arises due to a “phase transition”, where initial topology is overridden by added edges according to the associated  $\mathcal{D}_c$  target neighbor distributions. In the original graph, the homophily ratio is quite high ( $h = 0.85$ ), and classification behavior is akin to that discussed in Observation 1, where nodes with the same label have quite similar neighborhood patterns. As we add edges to the graph, the originally evident neighborhood patterns which benefited classification performance are perturbed by added edges and gradually become less informative, which leads to the performance decrease in the decreasing segment of the  $V$ -shape in Figure 3(a). Then, as we keep adding more edges, the neighborhood pattern gradually approaches  $\mathcal{D}_c$  for all  $c$ , corresponding to the increasing segment of the  $V$ -shape. As  $K \rightarrow \infty$ , neighborhood distributions will converge to the target  $\mathcal{D}_c$ , and classification accuracy will reach 100% (see Appendix C).

### 3.2.2 Introducing noise to neighborhood distributions

In Section 3.2.1, we showed that the GCN model can achieve reasonable performance on heterophilous graphs constructed following distinct, pre-defined neighborhood patterns. As per Observation 2, our theoretical understanding suggests that performance should degrade under heterophily if the distributions of different labels get more and more indistinguishable. Hence, we next demonstrate this empirically by introducing controllable noise levels into our edge addition strategy. We adopt a strategy similar to that described in Algorithm 1, but with the key difference being that we introduce an additional parameter  $\gamma$ , which controls the probability that we add cross-label edges *randomly* rather than following the pre-defined distribution  $\{\mathcal{D}_c, c \in \mathcal{C}\}$ . A detailed description of this approach is demonstrated in Algorithm 2 in Appendix C. For nodes of a given class  $c$  (w.l.o.g), compared to the edges added according to  $\mathcal{D}_c$ , the randomly added edges can be regarded as noise. Specifically, by increasing the noise parameter  $\gamma$ , we increase the similarity between  $\mathcal{D}_c, \mathcal{D}_{c'}$  for any pair of labels  $c, c'$ . If  $\gamma = 1$ , then all neighborhood distributions will be indistinguishable (they will all be approximately  $\text{Uniform}(|\mathcal{C}|)$ ). By fixing  $K$  and varying  $\gamma$ , we can generate graph variants with exactly the same homophily ratio but with differing similarities between  $\mathcal{D}_c$  and  $\mathcal{D}_{c'}$ . As in Section 3.2.1, we create graphs by adding edges at various  $K$ , but also vary  $\gamma \in [0, 1]$  in increments of 0.2 on both Cora and CiteSeer. We report the SSNC performance on these graphs in Figure 3.

We make several observations from the results: The noise level affects the performance significantly when the homophily ratio is low. For example, observing Figure 3(a) vertically at homophily ratio  $h = 0.3$ , higher  $\gamma$  clearly results in worse performance. This indicates that not only the fixed-ness of the neighborhood distributions, but their similarities are important for the SSNC task. It also indicates that there are “good” and “bad” kinds of heterophily; adding yet another supporting claim that heterophily is not the factor that determines whether GCNs work or fail for a certain graph. On the other hand, high  $\gamma$  does not too-negatively impact when  $K$  is small, since noise is minimal and the original graph topology is yet largely homophilous (when  $h$  is large, towards the left of the plot). At this stage, both “good” (fixed and disparate patterns) and “bad” (randomly added edges) heterophilous edges introduce noise to the dominant homophilous patterns which allow GCNs to separate classes well. When the noise level  $\gamma$  is not too large, we can still observe the  $V$ -shape: e.g.  $\gamma = 0.4$  in Figure 3(a) and  $\gamma = 0.2$  in Figure 3 (b); this is because the designed pattern is not totally

dominated by the noise. However, when  $\gamma$  is too high, adding edges will constantly decrease the performance, as nodes of different classes have indistinguishably similar neighborhoods.

To further demonstrate how  $\gamma$  affects the neighborhood distributions in the generated graph, we examine the cross-class neighborhood similarity, which we define as follows:

**Definition 2** (Cross-Class Neighborhood Similarity). *Given a graph  $\mathcal{G} = \{\mathcal{V}, \mathcal{E}\}$  and node labels  $\mathbf{y}$  for all nodes, the cross-class neighborhood similarity between classes  $c, c' \in \mathcal{C}$  is given by*

$$s(c, c') = \frac{1}{|\mathcal{V}_c||\mathcal{V}_{c'}|} \sum_{i \in \mathcal{V}_c, j \in \mathcal{V}_{c'}} \cos(d(i), d(j)) \quad (8)$$

where  $\mathcal{V}_c$  (w.l.o.g) indicates the set of nodes in class  $c$  and  $d(i)$  denotes the empirical histogram (over  $|\mathcal{C}|$  classes) of node  $i$ 's neighbors' labels, and the function  $\cos(\cdot, \cdot)$  measures the cosine similarity.

When  $c = c'$ ,  $s(c, c')$  calculates the intra-class similarity, otherwise, it calculates the inter-class similarity from a neighborhood label distribution perspective. Intuitively, if nodes with the same label share the same neighborhood distributions, the intra-class similarity should be high. Likewise, to ensure the neighborhood pattern for nodes with different labels are distinguishable, the inter-class similarity should be low. To illustrate how various  $\gamma$  values affect the neighborhood patterns, we illustrate the intra-class and inter-class similarities in Figure 4 for  $\gamma = 0, 0.4, 0.8, 1$  on graphs generated from Cora with homophily ratio  $h = 0.3$ . The diagonal cells in each heatmap indicate the intra-class similarity while off-diagonal cells indicate inter-class similarity. Clearly, when  $\gamma$  is small, the intra-class similarity is high while the inter-class similarity is low, which demonstrates the existence of strongly discriminative neighborhood patterns in the graph. As  $\gamma$  increases, the intra-class and inter-class similarity get closer, becoming more and more indistinguishable, leading to bad performance due to indistinguishable distributions as referenced in Observation 2.

## 4 Revisiting GCN's Performance on Real-world Graphs

How can we reconcile our findings with existing literature on GCN's performance under heterophily? As noted in Section 3, we observed that on some publicly available heterophilous graph benchmark datasets, the GCN model surprisingly outperforms methods specifically designed to deal with heterophilous graphs. In this section, we first give more details on these experiments. We next investigate why the GCN model does or does not work well on certain datasets utilizing the understanding developed in earlier sections.

### 4.1 Evaluating Node Classification on Homophilous and Heterophilous Benchmarks

Following previous work [26, 41], we evaluate the performance of the GCN model on several real-world graphs with different levels of homophily. We include the citation networks Cora, Citeseer and Pubmed [18], which are highly homophilous. We also adopt several heterophilous benchmark datasets including Chameleon, Squirrel, Actor, Cornell, Wisconsin and Texas [26]. Appendix D.1 gives descriptions and summary statistics of these datasets. For all datasets, we follow the experimental setting provided in [26], which consists of 10 random splits with proportions 48/32/20% corresponding to training/validation/test for each graph. For each split, we use 10 random seeds, and report the average performance and standard deviation across 100 runs. We compare the standard GCN model [18] with several recently proposed methods specifically designed for heterophilous graphs including H2GCN [41], GPR-GNN [4], and CPGNN [40]. A brief introduction of these methods can be found in Appendix D.2.

We carefully tuned the parameters for all models. The detailed parameter tuning settings can be found in Appendix D.4. The experimental setting in H2GCN [41] is the same as [26], hence we include the results for their method reported in the original paper.

The node classification performance (accuracy) of these models is reported in Table 2. Notably, all models achieve comparable performance on graphs with high homophily (Cora, Citeseer, and Pubmed), as expected. For the heterophilous graphs, results are comparatively mixed. The GCN model outperforms all other methods on Squirrel and Chameleon, while underperforming on the other datasets (Actor, Cornell, Wisconsin, and Texas). However, on these datasets, a two-layer feedforward model (denoted as MLP) always achieves comparable or even better performance than even the methods specifically designed for these graphs. Hence, we suspect that in these datasets, the graph offers un-useful (and sometimes actively damaging) information for node classification. Note that, both H2GCN and GPRGNN have skip connection (or similar architecture) to directly

Table 2: GNN node classification performance (accuracy) on homophilous and heterophilous graphs. Standard GCN or MLP+GCN methods (top) outperform or achieve comparable performance to heterophily-specific methods (bottom).

	Cora	Citeseer	Pubmed	Chameleon	Squirrel	Actor	Cornell	Wisconsin	Texas
GCN	$87.12 \pm 1.38$	$76.50 \pm 1.61$	$88.52 \pm 0.41$	$67.96 \pm 1.82$	$54.47 \pm 1.17$	$30.31 \pm 0.98$	$59.35 \pm 4.19$	$61.76 \pm 6.15$	$63.81 \pm 5.27$
MLP	$75.04 \pm 1.97$	$72.40 \pm 1.97$	$87.84 \pm 0.30$	$48.11 \pm 2.23$	$31.68 \pm 1.90$	$36.17 \pm 1.09$	<b><math>84.86 \pm 6.04</math></b>	$86.29 \pm 4.50$	$83.30 \pm 4.54$
MLP + GCN	$87.01 \pm 1.35$	$76.35 \pm 1.85$	<b><math>89.77 \pm 0.39</math></b>	<b><math>68.04 \pm 1.86</math></b>	<b><math>54.48 \pm 1.11</math></b>	<b><math>36.24 \pm 1.09</math></b>	$84.82 \pm 4.87$	$86.43 \pm 4.00$	$83.60 \pm 6.04$
H2GCN-1	$86.92 \pm 1.37$	$77.07 \pm 1.64$	$89.40 \pm 0.34$	$57.11 \pm 1.58$	$36.42 \pm 1.89$	$35.86 \pm 1.03$	$82.16 \pm 6.00$	<b><math>86.67 \pm 4.69</math></b>	<b><math>84.86 \pm 6.77</math></b>
H2GCN-2	<b><math>87.81 \pm 1.35</math></b>	<b><math>76.88 \pm 1.77</math></b>	$89.59 \pm 0.33$	$59.39 \pm 1.98$	$37.90 \pm 2.02$	$35.62 \pm 1.30$	$82.16 \pm 6.00$	$85.88 \pm 4.22$	$82.16 \pm 5.28$
CPGNN-MLP	$85.84 \pm 1.20$	$74.80 \pm 0.92$	$86.58 \pm 0.37$	$54.53 \pm 2.37$	$29.13 \pm 1.57$	$35.76 \pm 0.92$	$79.93 \pm 6.12$	$84.58 \pm 2.72$	$82.62 \pm 6.88$
CPGNN-Cheby	$87.23 \pm 1.31$	$76.64 \pm 1.43$	$88.41 \pm 0.33$	$65.17 \pm 3.17$	$29.25 \pm 4.17$	$34.28 \pm 0.77$	$75.08 \pm 7.51$	$79.19 \pm 2.80$	$75.96 \pm 5.66$
GPR-GNN	$86.79 \pm 1.27$	$75.55 \pm 1.56$	$86.79 \pm 0.55$	$66.31 \pm 2.05$	$50.56 \pm 1.51$	$33.94 \pm 0.95$	$79.27 \pm 6.03$	$83.73 \pm 4.02$	$84.43 \pm 4.10$

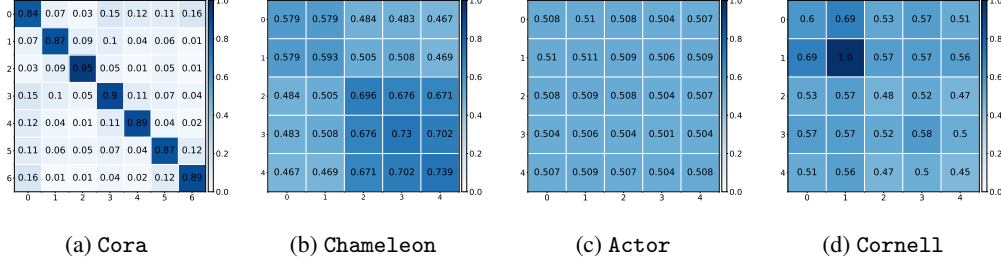


Figure 5: Cross-class neighborhood similarity on homophilous graphs (a) and heterophilous graphs (b-d). The deviations between inter and intra-class similarities substantiate GCN’s performance on these datasets.

connect the input features to the output. Their good performance on Actor, Cornell, Wisconsin, and Texas is likely attributed to this residual design. To verify this idea, we implement a simple method, which linearly combines the features output from GCN model and MLP model (denoted as MLP+GCN in Table 2; further details in Appendix D.3) and its performance is comparable or even better than heterophily-specific methods on all heterophilous graphs.

## 4.2 Investigating GCN performance on Homophilous and Heterophilous Benchmarks

Our work so far illustrates that the popular notion of GCNs not being suitable for heterophily, or homophily being a mandate for good GCN performance is not accurate. We believe this is due to prior evaluations having been conducted on a limited number of publicly available heterophilous graph benchmarks with relatively poor performance, which led to a (prima facie) conclusion that heterophily is the responsible for these issues rather than any of the other intrinsic properties of these datasets. In this subsection, we aim to use the understanding we developed in Section 3 to explain why GCN does (not) work well on real-world graphs. As in Section 3.2.2, we inspect cross-class neighborhood similarity (Eq.(8)) for each dataset; due to the space limit, we only include representative ones here (Cora, Chameleon, Actor and Cornell); see Figure 5). Heatmaps for the other datasets can be found in Appendix E. From Figure 5(a), it is clear that the intra-class similarity is much higher than the inter-similarity ones, hence Cora contains distinct neighborhood patterns, consistent with Observation 1. In Figure 5(b), we can observe that in Chameleon, intra-class similarity is generally higher than inter-class similarity, though not as strong as in Figure 5(a). Additionally, there is an apparent gap between labels 0, 1 and 2, 3, 4, which contributes in separating nodes of the former 2 from the latter 3 classes, but potentially increasing misclassification within each of the two groupings. These observations also help substantiate why GCN can achieve reasonable performance (much higher than MLP) on Chameleon. The GCN model underperforms MLP in Actor and we suspect that the graph does not provide useful information. The heatmap for Actor in Figure 5 shows that the intra-class and inter-class similarities are almost equivalent, making the neighborhood distributions for different classes hard to distinguish and leading to bad GCN performance. Similar observations can be made for Cornell. Note that Cornell only consists of 183 nodes and 280 edges, hence, the similarities shown in Figure 5 are impacted significantly by few samples (e.g. there is a single node with label 1, leading to perfect intra-class similarity for label 1).

## 5 Related Work

Graph neural networks (GNNs) are powerful models for graph representation learning. They have been widely adopted to tackle numerous applications from various domains [18, 8, 2, 31]. [29]

proposed the first GNN model, to tackle both node and graph level tasks. Subsequently, Bruna et al. [3] and Defferrard et al. [7] generalized convolutional neural networks to graphs from the graph spectral perspective. Kipf and Welling [18] simplified the spectral GNN model and proposed graph convolutional networks (GCNs). Since then, numerous GNN variants, which follow specific forms of feature transformation (linear layers) and aggregation have been proposed [34, 13, 11, 19]. The aggregation process can be usually understood as feature smoothing [20, 21, 16, 42]. Hence, several recent works claim [41, 40, 4], assume [12, 35, 38] or remark upon [1, 22, 14] GNN models homophily-reliance or unsuitability in capturing heterophily. Several recent works specifically develop GNN models choices to tackle heterophilous graphs by carefully designing or modifying model architectures such as Geom-GCN [26], H2GCN [41], GPR-GNN [4], and CPGNN [40].

## 6 Conclusion

It is widely believed that GNN models inherently assume strong homophily and hence fail to generalize to graphs with heterophily, hence performing poorly in SSNC tasks on heterophilous graphs. In this paper, we revisit this popular notion in literature, and show that it is not quite true. We investigate one representative model, GCN, and show empirically that it can achieve good performance on heterophilous graphs under certain conditions, sometimes better than more complex architectures specifically designed for such graphs (and indeed, correct the record for some common benchmark datasets). We next analyze theoretically what conditions are required for GCNs to learn similar embeddings for nodes of the same class, facilitating the SSNC task; put simply, when nodes with the same label share similar neighborhood patterns, and different classes have distinguishable patterns, GCN can achieve strong class separation, regardless of homophily or heterophily properties. Empirical analysis supports our theoretical findings. Finally, we revisit several existing homophilous and heterophilous SSNC benchmark graphs, and investigate GCN’s empirical performance in light of our understanding. Note that while we demonstrate that there exist graphs with “good heterophily”, the “bad heterophily” still poses challenges to GNN models, which calls for dedicated efforts.

Though we provide new perspectives and understandings of GCN’s performance on heterophilous graphs, our work has some limitations. Firstly, our current theoretical analysis majorly focuses on the GCN model; we hope to extend this analysis in the future to more general message-passing neural networks (MPNNs). Secondly, we plan to continue characterization of sufficient distinguishability of neighborhood and feature distributions to facilitate best class separation for future investigation.

## References

- [1] Sami Abu-El-Haija, Bryan Perozzi, Amol Kapoor, Nazanin Alipourfard, Kristina Lerman, Hrayr Harutyunyan, Greg Ver Steeg, and Aram Galstyan. MixHop: Higher-order graph convolutional architectures via sparsified neighborhood mixing. In Kamalika Chaudhuri and Ruslan Salakhutdinov, editors, *Proceedings of the 36th International Conference on Machine Learning*, volume 97 of *Proceedings of Machine Learning Research*, pages 21–29. PMLR, 09–15 Jun 2019. URL <http://proceedings.mlr.press/v97/abu-el-haija19a.html>.
- [2] Joost Bastings, Ivan Titov, Wilker Aziz, Diego Marcheggiani, and Khalil Sima’an. Graph convolutional encoders for syntax-aware neural machine translation. *arXiv preprint arXiv:1704.04675*, 2017.
- [3] Joan Bruna, Wojciech Zaremba, Arthur Szlam, and Yann LeCun. Spectral networks and locally connected networks on graphs. *arXiv preprint arXiv:1312.6203*, 2013.
- [4] Eli Chien, Jianhao Peng, Pan Li, and Olgica Milenkovic. Adaptive universal generalized pagerank graph neural network. In *International Conference on Learning Representations*, 2021. URL <https://openreview.net/forum?id=n6j17fLxrP>.
- [5] Valerio Ciotti, Moreno Bonaventura, Vincenzo Nicosia, Pietro Panzarasa, and Vito Latora. Homophily and missing links in citation networks. *EPJ Data Science*, 5:1–14, 2016.
- [6] Enyan Dai and Suhang Wang. Say no to the discrimination: Learning fair graph neural networks with limited sensitive attribute information. In *Proceedings of the 14th ACM International Conference on Web Search and Data Mining*, pages 680–688, 2021.
- [7] Michaël Defferrard, Xavier Bresson, and Pierre Vandergheynst. Convolutional neural networks on graphs with fast localized spectral filtering. *arXiv preprint arXiv:1606.09375*, 2016.

[8] Wenqi Fan, Yao Ma, Qing Li, Yuan He, Eric Zhao, Jiliang Tang, and Dawei Yin. Graph neural networks for social recommendation. In *The World Wide Web Conference*, pages 417–426, 2019.

[9] Ronald A Fisher. The use of multiple measurements in taxonomic problems. *Annals of eugenics*, 7(2):179–188, 1936.

[10] Elisabeth R Gerber, Adam Douglas Henry, and Mark Lubell. Political homophily and collaboration in regional planning networks. *American Journal of Political Science*, 57(3):598–610, 2013.

[11] Justin Gilmer, Samuel S Schoenholz, Patrick F Riley, Oriol Vinyals, and George E Dahl. Neural message passing for quantum chemistry. In *International Conference on Machine Learning*, pages 1263–1272. PMLR, 2017.

[12] Jonathan Halcrow, Alexandru Mosoi, Sam Ruth, and Bryan Perozzi. Grale: Designing networks for graph learning. In *Proceedings of the 26th ACM SIGKDD International Conference on Knowledge Discovery & Data Mining*, pages 2523–2532, 2020.

[13] William L Hamilton, Rex Ying, and Jure Leskovec. Inductive representation learning on large graphs. *arXiv preprint arXiv:1706.02216*, 2017.

[14] Yifan Hou, Jian Zhang, James Cheng, Kaili Ma, Richard T. B. Ma, Hongzhi Chen, and Ming-Chang Yang. Measuring and improving the use of graph information in graph neural networks. In *International Conference on Learning Representations*, 2020. URL <https://openreview.net/forum?id=rkeIIkHKvS>.

[15] Ankit Jain and Piero Molino. Enhancing recommendations on uber eats with graph convolutional networks.

[16] Junteng Jia and Austin R Benson. A unifying generative model for graph learning algorithms: Label propagation, graph convolutions, and combinations. *arXiv preprint arXiv:2101.07730*, 2021.

[17] Weiwei Jiang and Jiayun Luo. Graph neural network for traffic forecasting: A survey. *arXiv preprint arXiv:2101.11174*, 2021.

[18] Thomas N Kipf and Max Welling. Semi-supervised classification with graph convolutional networks. *arXiv preprint arXiv:1609.02907*, 2016.

[19] Johannes Klicpera, Aleksandar Bojchevski, and Stephan Günnemann. Predict then propagate: Graph neural networks meet personalized pagerank. In *International Conference on Learning Representations (ICLR)*, 2019.

[20] Qimai Li, Zhichao Han, and Xiao-Ming Wu. Deeper insights into graph convolutional networks for semi-supervised learning. In *Proceedings of the AAAI Conference on Artificial Intelligence*, volume 32, 2018.

[21] Yao Ma, Xiaorui Liu, Tong Zhao, Yozen Liu, Jiliang Tang, and Neil Shah. A unified view on graph neural networks as graph signal denoising. *arXiv preprint arXiv:2010.01777*, 2020.

[22] Sunil Kumar Maurya, Xin Liu, and Tsuyoshi Murata. Improving graph neural networks with simple architecture design. *arXiv preprint arXiv:2105.07634*, 2021.

[23] Miller McPherson, Lynn Smith-Lovin, and James M Cook. Birds of a feather: Homophily in social networks. *Annual review of sociology*, 27(1):415–444, 2001.

[24] Christopher Morris, Martin Ritzert, Matthias Fey, William L Hamilton, Jan Eric Lenssen, Gaurav Rattan, and Martin Grohe. Weisfeiler and leman go neural: Higher-order graph neural networks. In *Proceedings of the AAAI Conference on Artificial Intelligence*, volume 33, pages 4602–4609, 2019.

[25] Mark Newman. *Networks*. Oxford university press, 2018.

[26] Hongbin Pei, Bingzhe Wei, Kevin Chen-Chuan Chang, Yu Lei, and Bo Yang. Geom-gcn: Geometric graph convolutional networks. In *International Conference on Learning Representations*, 2020. URL <https://openreview.net/forum?id=S1e2agrFvS>.

[27] Aravind Sankar, Yozen Liu, Jun Yu, and Neil Shah. Graph neural networks for friend ranking in large-scale social platforms. 2021.

[28] Kevin Scaman and Aladin Virmaux. Lipschitz regularity of deep neural networks: analysis and efficient estimation. *arXiv preprint arXiv:1805.10965*, 2018.

[29] Franco Scarselli, Marco Gori, Ah Chung Tsoi, Markus Hagenbuchner, and Gabriele Monfardini. The graph neural network model. *IEEE transactions on neural networks*, 20(1):61–80, 2008.

[30] Prithviraj Sen, Galileo Namata, Mustafa Bilgic, Lise Getoor, Brian Galligher, and Tina Eliassi-Rad. Collective classification in network data. *AI magazine*, 29(3):93–93, 2008.

[31] Lei Shi, Yifan Zhang, Jian Cheng, and Hanqing Lu. Skeleton-based action recognition with directed graph neural networks. In *Proceedings of the IEEE/CVF Conference on Computer Vision and Pattern Recognition*, pages 7912–7921, 2019.

[32] Xianfeng Tang, Yozen Liu, Neil Shah, Xiaolin Shi, Prasenjit Mitra, and Suhang Wang. Knowing your fate: Friendship, action and temporal explanations for user engagement prediction on social apps. In *Proceedings of the 26th ACM SIGKDD International Conference on Knowledge Discovery & Data Mining*, pages 2269–2279, 2020.

[33] Xianfeng Tang, Huaxiu Yao, Yiwei Sun, Yiqi Wang, Jiliang Tang, Charu Aggarwal, Prasenjit Mitra, and Suhang Wang. Investigating and mitigating degree-related biases in graph convolutional networks. In *Proceedings of the 29th ACM International Conference on Information & Knowledge Management*, pages 1435–1444, 2020.

[34] Petar Veličković, Guillem Cucurull, Arantxa Casanova, Adriana Romero, Pietro Lio, and Yoshua Bengio. Graph attention networks. *arXiv preprint arXiv:1710.10903*, 2017.

[35] Xuan Wu, Lingxiao Zhao, and Leman Akoglu. A quest for structure: jointly learning the graph structure and semi-supervised classification. In *Proceedings of the 27th ACM international conference on information and knowledge management*, pages 87–96, 2018.

[36] Keyulu Xu, Weihua Hu, Jure Leskovec, and Stefanie Jegelka. How powerful are graph neural networks? In *International Conference on Learning Representations*, 2019. URL <https://openreview.net/forum?id=ryGs6ia5Km>.

[37] Rex Ying, Ruining He, Kaifeng Chen, Pong Eksombatchai, William L Hamilton, and Jure Leskovec. Graph convolutional neural networks for web-scale recommender systems. In *Proceedings of the 24th ACM SIGKDD International Conference on Knowledge Discovery & Data Mining*, pages 974–983, 2018.

[38] Tong Zhao, Yozen Liu, Leonardo Neves, Oliver Woodford, Meng Jiang, and Neil Shah. Data augmentation for graph neural networks. In *AAAI*, 2020.

[39] Jie Zhou, Ganqu Cui, Shengding Hu, Zhengyan Zhang, Cheng Yang, Zhiyuan Liu, Lifeng Wang, Changcheng Li, and Maosong Sun. Graph neural networks: A review of methods and applications. *AI Open*, 1:57–81, 2020.

[40] Jiong Zhu, Ryan A Rossi, Anup Rao, Tung Mai, Nedim Lipka, Nesreen K Ahmed, and Danai Koutra. Graph neural networks with heterophily. *arXiv preprint arXiv:2009.13566*, 2020.

[41] Jiong Zhu, Yujun Yan, Lingxiao Zhao, Mark Heimann, Leman Akoglu, and Danai Koutra. Beyond homophily in graph neural networks: Current limitations and effective designs. *Advances in Neural Information Processing Systems*, 33, 2020.

[42] Meiqi Zhu, Xiao Wang, Chuan Shi, Houye Ji, and Peng Cui. Interpreting and unifying graph neural networks with an optimization framework. *arXiv preprint arXiv:2101.11859*, 2021.

[43] Marinka Zitnik, Monica Agrawal, and Jure Leskovec. Modeling polypharmacy side effects with graph convolutional networks. *Bioinformatics*, 34(13):i457–i466, 2018.

## A Proof of Theorem 1

To prove Theorem 1, we first introduce the celebrated Hoeffding inequality below.

**Lemma 1** (Hoeffding's Inequality). *Let  $Z_1, \dots, Z_n$  be independent bounded random variables with  $Z_i \in [a, b]$  for all  $i$ , where  $-\infty < a \leq b < \infty$ . Then*

$$\mathbb{P} \left( \frac{1}{n} \sum_{i=1}^n (Z_i - \mathbb{E}[Z_i]) \geq t \right) \leq \exp \left( -\frac{2nt^2}{(b-a)^2} \right)$$

and

$$\mathbb{P} \left( \frac{1}{n} \sum_{i=1}^n (Z_i - \mathbb{E}[Z_i]) \leq -t \right) \leq \exp \left( -\frac{2nt^2}{(b-a)^2} \right)$$

for all  $t \geq 0$ .

**Theorem 1.** *Consider a graph  $\mathcal{G} = \{\mathcal{V}, \mathcal{E}, \{\mathcal{F}_c, c \in \mathcal{C}\}, \{\mathcal{D}_c, c \in \mathcal{C}\}, d\}$ , which follows Assumptions (1)-(5). For any node  $i \in \mathcal{V}$ , the expectation of its pre-activation output of 1-layer GCN model is as follows:*

$$\mathbb{E}[\mathbf{h}_i] = \mathbf{W} \left( \frac{1}{d+1} \mu(\mathcal{F}_{y_i}) + \frac{d}{d+1} \mathbb{E}_{c \sim \mathcal{D}_{y_i}, \mathbf{x} \sim \mathcal{F}_c} [\mathbf{x}] \right). \quad (9)$$

For any  $t > 0$ , the probability that the distance between the observation  $\mathbf{h}_i$  and its expectation is larger than  $t$  is bounded as follows.

$$\mathbb{P} (\|\mathbf{h}_i - \mathbb{E}[\mathbf{h}_i]\|_2 \geq t) \leq 2 \cdot l \cdot \exp \left( -\frac{(d+1)t^2}{2\rho^2(\mathbf{W})B^2l} \right), \quad (10)$$

where  $l$  is the dimension of features,  $\rho(\mathbf{W})$  denotes the largest singular value of  $\mathbf{W}$  and  $B$  is a bound for the features as introduced in **Assumptions on Graphs**.

*Proof.* The expectation of  $\mathbf{h}_i$  can be derived as follows.

$$\begin{aligned} \mathbb{E}[\mathbf{h}_i] &= \mathbb{E} \left[ \sum_{j \in \{i\} \cup \mathcal{N}(i)} \frac{1}{d+1} \mathbf{W} \mathbf{x}_j \right] \\ &= \frac{1}{d+1} \mathbf{W} \mathbb{E}[\mathbf{x}_i] + \sum_{j \in \mathcal{N}(i)} \frac{1}{d+1} \mathbf{W} \mathbb{E}[\mathbf{x}_j] \\ &= \frac{1}{d+1} \mathbf{W} \mu(\mathcal{F}_{y_i}) + \sum_{j \in \mathcal{N}(i)} \mathbf{W} \mathbb{E}_{c \sim \mathcal{D}_{y_i}, \mathbf{x} \sim \mathcal{F}_c} [\mathbf{x}] \\ &= \mathbf{W} \left( \frac{1}{d+1} \mu(\mathcal{F}_{y_i}) + \frac{d}{d+1} \mathbb{E}_{c \sim \mathcal{D}_{y_i}, \mathbf{x} \sim \mathcal{F}_c} [\mathbf{x}] \right). \end{aligned}$$

We utilize Hoeffding's Inequality to prove the bound in Eq. (10). Let  $\mathbf{x}_i[k], k = 1, \dots, l$  denote the  $i$ -th element of  $\mathbf{x}$ . Then, for any dimension  $k$ ,  $\{\mathbf{x}_j[k], j \in \mathcal{N}(i)\}$  is a set of independent bounded random variables. Hence, directly applying Hoeffding's inequality, for any  $t_1 \geq 0$ , we have the following bound:

$$\mathbb{P} \left( \left| \sum_{j \in \{i\} \cup \mathcal{N}(i)} (\mathbf{x}_j[k] - \mathbb{E}[\mathbf{x}_j[k]]) \right| \geq t_1 \right) \leq 2 \exp \left( -\frac{(d+1)t_1^2}{2B^2} \right)$$

If  $\left\| \sum_{j \in \{i\} \cup \mathcal{N}(i)} (\mathbf{x}_j - \mathbb{E}[\mathbf{x}_j]) \right\|_2 \geq \sqrt{l}t_1$ , then at least for one  $k \in \{1, \dots, l\}$ , the inequality

$\left| \sum_{j \in \{i\} \cup \mathcal{N}(i)} (\mathbf{x}_j[k] - \mathbb{E}[\mathbf{x}_j[k]]) \right| \geq t_1$  holds. Hence, we have

$$\mathbb{P} \left( \left\| \sum_{j \in \{i\} \cup \mathcal{N}(i)} (\mathbf{x}_j - \mathbb{E}[\mathbf{x}_j]) \right\|_2 \geq \sqrt{l}t_1 \right) \leq \mathbb{P} \left( \bigcup_{k=1}^l \left\{ \left| \sum_{j \in \{i\} \cup \mathcal{N}(i)} (\mathbf{x}_j[k] - \mathbb{E}[\mathbf{x}_j[k]]) \right| \geq t_1 \right\} \right)$$

$$\begin{aligned}
&\leq \sum_{k=1}^l \mathbb{P} \left( \left| \sum_{j \in \{i\} \cup \mathcal{N}(i)} (\mathbf{x}_j[k] - \mathbb{E}[\mathbf{x}_j[k]]) \right| \geq t_1 \right) \\
&= 2 \cdot l \cdot \exp \left( -\frac{(d+1)t_1^2}{2B^2} \right)
\end{aligned}$$

Let  $t_1 = \frac{t_2}{\sqrt{l}}$ , then we have

$$\mathbb{P} \left( \left\| \sum_{j \in \{i\} \cup \mathcal{N}(i)} (\mathbf{x}_j - \mathbb{E}[\mathbf{x}_j]) \right\|_2 \geq t_2 \right) \leq 2 \cdot l \cdot \exp \left( -\frac{(d+1)t_2^2}{2B^2l} \right)$$

Furthermore, we have

$$\begin{aligned}
\|\mathbf{h}_i - \mathbb{E}[\mathbf{h}_i]\|_2 &= \left\| \mathbf{W} \left( \sum_{j \in \{i\} \cup \mathcal{N}(i)} (\mathbf{x}_j - \mathbb{E}[\mathbf{x}_j]) \right) \right\|_2 \\
&\leq \|\mathbf{W}\|_2 \left\| \sum_{j \in \{i\} \cup \mathcal{N}(i)} (\mathbf{x}_j - \mathbb{E}[\mathbf{x}_j]) \right\|_2 \\
&= \rho(\mathbf{W}) \left\| \sum_{j \in \{i\} \cup \mathcal{N}(i)} (\mathbf{x}_j - \mathbb{E}[\mathbf{x}_j]) \right\|_2,
\end{aligned}$$

where  $\|\mathbf{W}\|_2$  is the matrix 2-norm of  $\mathbf{W}$ . Note that the last line uses the identity  $\|\mathbf{W}\|_2 = \rho(\mathbf{W})$ .

Then, for any  $t > 0$ , we have

$$\begin{aligned}
\mathbb{P}(\|\mathbf{h}_i - \mathbb{E}[\mathbf{h}_i]\|_2 \geq t) &\leq \mathbb{P} \left( \rho(\mathbf{W}) \left\| \sum_{j \in \{i\} \cup \mathcal{N}(i)} (\mathbf{x}_j - \mathbb{E}[\mathbf{x}_j]) \right\|_2 \geq t \right) \\
&= \mathbb{P} \left( \left\| \sum_{j \in \{i\} \cup \mathcal{N}(i)} (\mathbf{x}_j - \mathbb{E}[\mathbf{x}_j]) \right\|_2 \geq \frac{t}{\rho(\mathbf{W})} \right) \\
&\leq 2 \cdot l \cdot \exp \left( -\frac{(d+1)t^2}{2\rho^2(\mathbf{W})B^2l} \right),
\end{aligned}$$

which completes the proof.  $\square$

## B Proof of Theorem 2

**Theorem 2.** Consider a graph  $\mathcal{G} = \{\mathcal{V}, \mathcal{E}, \{\mathcal{F}_c, c \in \mathcal{C}\}, \{\mathcal{D}_c, c \in \mathcal{C}\}, d\}$ , which follows Assumptions (1)-(5). For any two nodes  $i, j \in \mathcal{V}$  that share the same label, i.e.,  $y_i = y_j$ , the probability that the distance between their output pre-activation embeddings (from eq. (4)) is larger than  $t$  ( $t > 0$ ) is bounded as follows.

$$\mathbb{P}(\|\mathbf{h}_i - \mathbf{h}_j\|_2 \geq t) \leq 4 \cdot l \cdot \exp \left( -\frac{(d+1)t^2}{8\rho^2(\mathbf{W})B^2l} \right) \quad (11)$$

*Proof.* If  $\|\mathbf{h}_i - \mathbf{h}_j\|_2 \geq t$ , then, at least one of the following two inequalities holds.

$$\begin{aligned}
\|\mathbf{h}_i - \mathbb{E}[\mathbf{h}_i]\|_2 &\geq \frac{t}{2} \\
\|\mathbf{h}_j - \mathbb{E}[\mathbf{h}_j]\|_2 &\geq \frac{t}{2}
\end{aligned}$$

Hence, we have

$$\begin{aligned}
\mathbb{P}(\|\mathbf{h}_i - \mathbf{h}_j\|_2 \geq t) &\leq \mathbb{P} \left( \left\{ \|\mathbf{h}_i - \mathbb{E}[\mathbf{h}_i]\|_2 \geq \frac{t}{2} \right\} \cup \left\{ \|\mathbf{h}_j - \mathbb{E}[\mathbf{h}_j]\|_2 \geq \frac{t}{2} \right\} \right) \\
&\leq \mathbb{P} \left( \|\mathbf{h}_i - \mathbb{E}[\mathbf{h}_i]\|_2 \geq \frac{t}{2} \right) + \mathbb{P} \left( \|\mathbf{h}_j - \mathbb{E}[\mathbf{h}_j]\|_2 \geq \frac{t}{2} \right)
\end{aligned}$$

$$\leq 4 \cdot l \cdot \exp\left(-\frac{(d+1)t^2}{8\rho^2(\mathbf{W})\mathbf{B}^2l}\right)$$

□

## C Additional Details and Results for Section 3.2.1

### C.1 Details on the generated graphs

In this subsection, we present the details of the graphs that we generate in Section 3.2.1. Specifically, we detail the distributions  $\{\mathcal{D}_c, c \in \mathcal{C}\}$  used in the examples, the number of added edges  $K$ , and the homophily ratio  $h$ . We provide the details for **Cora** and **Citeseer** in the following subsections. Note that the choices of distributions shown here are for illustrative purposes, to coincide with Observations 1 and 2. We adapted circulant matrix-like designs due to their simplicity.

#### C.1.1 Cora

There are 7 labels, which we denote as  $\{0, 1, 2, 3, 4, 5, 6\}$ . The distributions  $\{\mathcal{D}_c, c \in \mathcal{C}\}$  are listed as follows. The values of  $K$  and the homophily ratio of their corresponding generated graphs are shown in Table 3.

$$\begin{aligned}\mathcal{D}_0 &: \text{Categorical}([0, 0.5, 0, 0, 0, 0, 0.5]), \\ \mathcal{D}_1 &: \text{Categorical}([0.5, 0, 0.5, 0, 0, 0, 0]), \\ \mathcal{D}_2 &: \text{Categorical}([0, 0.5, 0, 0.5, 0, 0, 0]), \\ \mathcal{D}_3 &: \text{Categorical}([0, 0, 0.5, 0, 0.5, 0, 0]), \\ \mathcal{D}_4 &: \text{Categorical}([0, 0, 0, 0.5, 0, 0.5, 0]), \\ \mathcal{D}_5 &: \text{Categorical}([0, 0, 0, 0, 0.5, 0, 0.5]), \\ \mathcal{D}_6 &: \text{Categorical}([0.5, 0, 0, 0, 0, 0.5, 0]).\end{aligned}$$

Table 3:  $K$  and  $h$  values for generated graphs based on **Cora**

$K$	1003	2006	3009	4012	6018	8024	10030	12036	16048	20060	24072
$h$	0.789	0.737	0.692	0.652	0.584	0.529	0.483	0.445	0.384	0.338	0.302

#### C.1.2 Citeseer

There are 6 labels, which we denote as  $\{0, 1, 2, 3, 4, 5\}$ . The distributions  $\{\mathcal{D}_c, c \in \mathcal{C}\}$  are listed as follows. The values of  $K$  and the homophily ratio of their corresponding generated graphs are shown in Table 4.

$$\begin{aligned}\mathcal{D}_0 &: \text{Categorical}([0, 0.5, 0, 0, 0, 0.5]), \\ \mathcal{D}_1 &: \text{Categorical}([0.5, 0, 0.5, 0, 0, 0]), \\ \mathcal{D}_2 &: \text{Categorical}([0, 0.5, 0, 0.5, 0, 0]), \\ \mathcal{D}_3 &: \text{Categorical}([0, 0, 0.5, 0, 0.5, 0]), \\ \mathcal{D}_4 &: \text{Categorical}([0, 0, 0, 0.5, 0, 0.5]), \\ \mathcal{D}_5 &: \text{Categorical}([0.5, 0, 0, 0, 0.5, 0]).\end{aligned}$$

Table 4:  $K$  and  $h$  values for generated graphs based on **Citeseer**

$K$	1204	2408	3612	4816	7224	9632	12040	14448	19264	24080	28896
$h$	0.735	0.675	0.625	0.581	0.510	0.454	0.410	0.373	0.316	0.275	0.243

### C.2 Results on more datasets: Chameleon and Squirrel

We conduct similar experiments as those in Section 3.2.1 based on **Chameleon** and **Squirrel**. Note that both **Squirrel** and **Chameleon** have 5 labels, which we denote as  $\{0, 1, 2, 3, 4\}$ . We pre-define

the same distributions for them as listed as follows. The values of  $K$  and the homophily ratio of their corresponding generated graphs based on *Squirrel* and *Chameleon* are shown in Table 5 and Table 6, respectively.

$$\begin{aligned}
\mathcal{D}_0 &: \text{Categorical}([0, 0.5, 0, 0, 0.5]), \\
\mathcal{D}_1 &: \text{Categorical}([0.5, 0, 0.5, 0, 0]), \\
\mathcal{D}_2 &: \text{Categorical}([0, 0.5, 0, 0.5, 0]), \\
\mathcal{D}_3 &: \text{Categorical}([0, 0, 0.5, 0, 0.5]), \\
\mathcal{D}_4 &: \text{Categorical}([0.5, 0, 0, 0.5, 0]). \\
\end{aligned} \tag{12}$$

Table 5:  $K$  and  $h$  values for generated graphs based on *Squirrel*

$K$	12343	24686	37030	49374	61716	74060	86404	98746	111090	12434	135776
$h$	0.232	0.225	0.219	0.207	0.201	0.196	0.191	0.186	0.181	0.178	0.174

Table 6:  $K$  and  $h$  values for generated graphs based on *Chameleon*

K	1932	3866	5798	7730	9964	11596	13528	15462	17394	19326	21260
Homo. Ratio	0.249	0.242	0.236	0.230	0.224	0.218	0.213	0.208	0.203	0.198	0.194

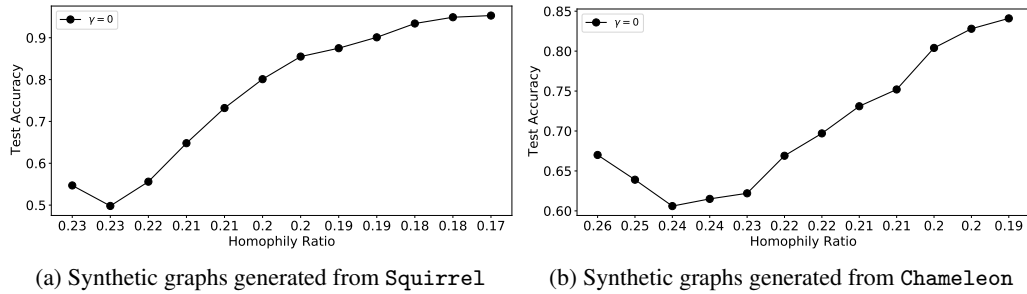


Figure 6: Performance of GCN on synthetic graphs with various homophily ratio.

The performance of the GCN model on these two sets of graphs (generated from *Squirrel* and *Chameleon*) is shown in Figure 6. The observations are similar to what we found for those generated graphs based on *Cora* and *Citeseer* in Section 3.2.1. Note that the original *Squirrel* and *Chameleon* graphs already have very low homophily, but we still observe a  $V$ -shape from the figures. This is because there are some neighborhood patterns in the original graphs, which are distinct from those that we designed for addition. Hence, when we add edges in the early stage, the performance decreases. As we add more edges, the designed pattern starts to mask the original patterns and the performance starts to increase.

### C.3 GCN’s Performance in the Limit (as $K \rightarrow \infty$ )

In this subsection, we illustrate that as  $K \rightarrow \infty$ , the accuracy of the GCN model approaches 100%. Specifically, we set  $K$  to a set of larger numbers as listed in Table 7. Ideally, when  $K \rightarrow \infty$ , the homophily ratio will approach 0 and the model performance will approach 100% (for diverse-enough  $\mathcal{D}_c$ ). The performance of the GCN model on the graphs described in Table 3 and Table 7 are shown in Figure 7. Clearly, the performance of the GCN model approaches the maximum as we continue to increase  $K$ .

Table 7: Extended  $K$  and  $h$  values for generated graphs based on Cora

$K$	28084	32096	36108	40120	44132	48144	52156	56168	80240
$h$	0.272	0.248	0.228	0.211	0.196	0.183	0.172	0.162	0.120

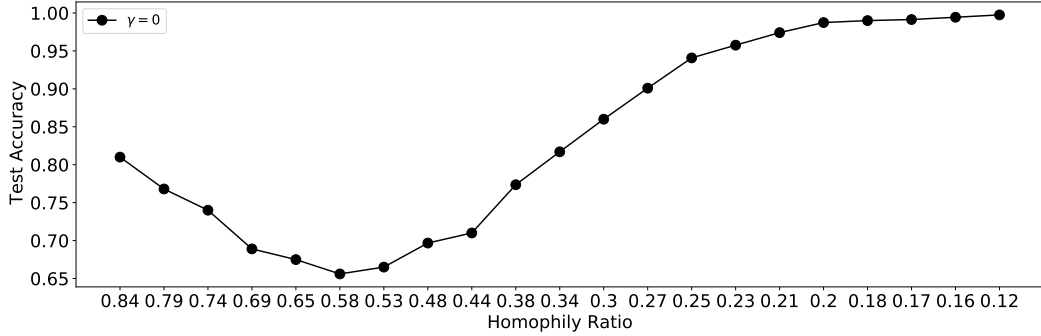


Figure 7: The GCN’s performance approaches 100% as we keep adding edges following the specific patterns

#### C.4 Details of Algorithm 2

The pseudo code to describe the process to generate graphs with a noise level  $\gamma$  is shown in Algorithm 2. The only difference from Algorithm 1 is in Line 6-7, we randomly add edges if the generated random number  $r$  is smaller than the pre-defined  $\gamma$  (with probability  $\gamma$ ).

---

#### Algorithm 2: Heterophilous Edge Addition with Noise

---

```

input :  $\mathcal{G} = \{\mathcal{V}, \mathcal{E}\}$ ,  $K$ ,  $\{\mathcal{D}_c\}_{c=0}^{|\mathcal{C}|-1}$  and  $\{\mathcal{V}_c\}_{c=0}^{|\mathcal{C}|-1}$ 
output :  $\mathcal{G}' = \{\mathcal{V}, \mathcal{E}'\}$ 
Initialize  $\mathcal{G}' = \{\mathcal{V}, \mathcal{E}\}$ ,  $k = 1$  ;
while  $1 \leq k \leq K$  do
    Sample node  $i \sim \text{Uniform}(\mathcal{V})$ ;
    Obtain the label,  $y_i$  of node  $i$ ;
    Sample a number  $r \sim \text{Uniform}(0,1)$  ; // Uniform(0,1) denotes the continuous standard uniform distribution
    if  $r \leq \gamma$  then
        Sample a label  $c \sim \text{Uniform}(\mathcal{C} \setminus \{y_i\})$ ;
    else
        Sample a label  $c \sim \mathcal{D}_{y_i}$ ;
    Sample node  $j \sim \text{Uniform}(\mathcal{V}_c)$ ;
    Update edge set  $\mathcal{E}' = \mathcal{E}' \cup \{(i, j)\}$ ;
     $k \leftarrow k + 1$ ;
return  $\mathcal{G}' = \{\mathcal{V}, \mathcal{E}'\}$ 

```

---

## D Experimental Settings: Datasets and Models

### D.1 Datasets

We give the number of nodes, edges, homophily ratios and distinct classes of datasets we used in this paper in Table 8.

Table 8: Benchmark dataset summary statistics.

	Cora	Citeseer	Pubmed	Chameleon	Squirrel	Actor	Cornell	Wisconsin	Texas
# Nodes ( $ \mathcal{V} $ )	2708	3327	19717	2277	5201	7600	183	251	183
# Edges ( $ \mathcal{E} $ )	5278	4676	44327	31421	198493	26752	280	466	295
Homophily Ratio ( $h$ )	0.81	0.74	0.80	0.23	0.22	0.22	0.3	0.21	0.11
# Classes ( $ \mathcal{C} $ )	7	6	3	5	5	5	5	5	5

## D.2 Models

- H2GCN [41] specifically designed several architectures to deal with heterophilous graphs, which include ego- and neighbor-embedding separation (skip connection), aggregation from higher-order neighborhoods, and combination of intermediate representations. We include two variants H2GCN-1 and H2GCN-2 with 1 or 2 steps of aggregations, respectively. We adopt the code published by the authors at <https://github.com/GemsLab/H2GCN>.
- GPR-GNN [4] performs feature aggregation for multiple steps and then linearly combines the features aggregated with different steps. The weights of the linear combination are learned during the model training. Note that it also includes the original features before aggregation in the combination. We adopt the code published by the authors at <https://github.com/jianhao2016/GPRGNN>.
- CPGNN [40] incorporates the label compatibility matrix to capture the connection information between classes. We adopted two variants of CPGNN that utilize MLP and ChebyNet [7] as base models to pre-calculate the compatibility matrix, respectively. We use two aggregation layers for both variants. We adopt the code published by the authors at <https://github.com/GemsLab/CPGNN>.

## D.3 MLP+GCN

We implement a simple method to linearly combine the learned features from the GCN model and an MLP model. Let  $\mathbf{H}_{GCN}^{(2)} \in \mathbb{R}^{|\mathcal{V}| \times |\mathcal{C}|}$  denote the output features from a 2-layer GCN model, where  $|\mathcal{V}|$  and  $|\mathcal{C}|$  denote the number of nodes and the number of classes, respectively. Similarly, we use  $\mathbf{H}_{MLP}^{(2)} \in \mathbb{R}^{|\mathcal{V}| \times |\mathcal{C}|}$  to denote the features output from a 2-layer MLP model. We then combine them for classification. The process can be described as follows.

$$\mathbf{H} = \alpha \cdot \mathbf{H}_{GCN}^{(2)} + (1 - \alpha) \cdot \mathbf{H}_{MLP}^{(2)}, \quad (13)$$

where  $\alpha$  is a hyperparameter balancing the two components. We then apply a row-wise softmax to each row of  $\mathbf{H}$  to perform the classification.

## D.4 Parameter Tuning and Resources Used

We tune parameters for GCN, GPR-GCN, CPGNN, and MLP+GCN from the following options:

- learning rate:  $\{0.002, 0.005, 0.01, 0.05\}$
- weight decay  $\{5e-04, 5e-05, 5e-06, 5e-07, 5e-08, 1e-05, 0\}$
- dropout rate:  $\{0, 0.2, 0.5, 0.8\}$ .

For GPR-GNN, we use the “PPR” as the initialization for the coefficients. For MLP+GCN, we tune  $\alpha$  from  $\{0.2, 0.4, 0.6, 0.8, 1\}$ . Note that the parameter search range encompasses the range adopted in the original papers to avoid unfairness issues.

All experiments are run on a cluster equipped with *Intel(R) Xeon(R) CPU E5-2680 v4 @ 2.40GHz* CPUs and *NVIDIA Tesla K80* GPUs.

## E Heatmaps for Other Benchmarks

We provide the heatmaps for Citeseer and Pubmed in Figure 8 and those for Squirrel, Texas, and Wisconsin in Figure 9. For the Citeseer and Pubmed, which have high homophily, the observations are similar to those of Cora as we described in Section 4.2. For Squirrel, there are some patterns; the intra-class similarity is generally higher than inter-class similarities. However, these patterns are not very strong, i.e, the differences between them are not very large, which means that the neighborhood patterns of different labels are not very distinguishable from each other. This substantiates the middling performance of GCN on Squirrel. Both Texas and Wisconsin are very small, with 183 nodes, 295 edges and 251 nodes, 466 edges, respectively. The average degree is extremely small ( $< 2$ ). Hence, the similarities presented in the heatmap may present strong bias. Especially, in Texas, there is only 1 node with label 1. In Wisconsin, there are only 10 nodes with label 0.

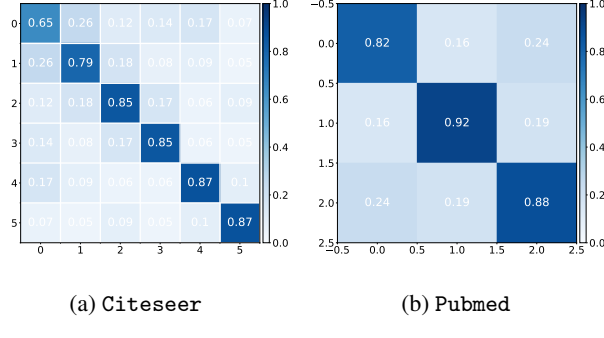


Figure 8: Neighborhood Similarity On CiteSeer and Pubmed. On both graphs, the intra-class similarity is clearly higher than the inter-class ones.

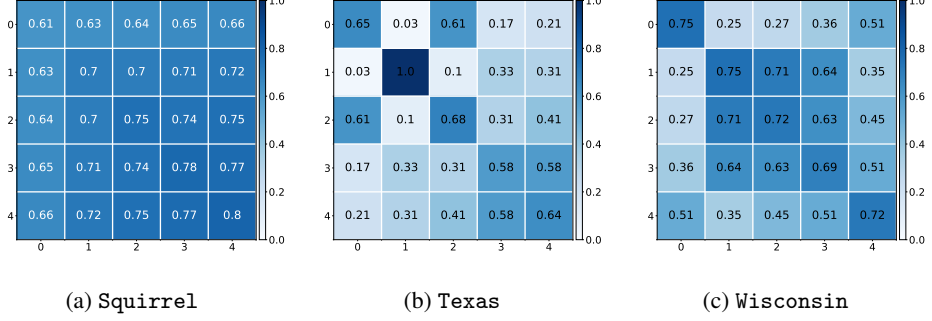


Figure 9: Neighborhood Similarity On Squirrel, Texas and Wisconsin. The inter-class similarity on Squirrel is slightly higher than intra-class similarity for most classes, which substantiates the middling performance of GCN. Both Texas and Wisconsin are quite small, hence the cross-class similarity in these two graphs present severe bias and may not provide precise information about these graphs.

## F Broader Impact

Graph neural networks (GNNs) are a prominent architecture for modeling and understanding graph-structured data in a variety of practical applications. Most GNNs have a natural inductive bias towards leveraging graph neighborhood information to make inferences, which can exacerbate unfair or biased outcomes during inference, especially when such neighborhoods are formed according to inherently biased upstream processes, e.g. rich-get-richer phenomena and other disparities in the opportunities to “connect” to other nodes: For example, older papers garner more citations than newer ones, and are hence likely to have a higher in-degree in citation networks and hence benefit more from neighborhood information; similar analogs can be drawn for more established webpages attracting more attention in search results. Professional networking (“ability to connect”) may be easier for those individuals (nodes) who are at top-tier, well-funded universities compared to those who are not. Such factors influence network formation, sparsity, and thus GNN inference quality simply due to network topology [33]. Given these acknowledged issues, GNNs are still used in applications including ranking [27], recommendation[15], engagement prediction [32], traffic modeling[17], search and discovery [37] and more, and when unchecked, suffer traditional machine learning unfairness issues [6].

Despite these practical impacts, the prominent notion in prior literature in this space has been that such methods are inapplicable or perform poorly on heterophilous graphs, and this may have mitigated practitioners’ interests in applying such methods for ML problems in those domains conventionally considered heterophily-dominant (e.g. dating networks). Our work shows that this notion is misleading, and that heterophily and homophily are not themselves responsible for good

or bad inference performance. We anticipate this finding to be helpful in furthering research into the capacity of GNN models to work in diverse data settings, and emphasize that our work provides an understanding, rather than a new methodology or approach, and thus do not anticipate negative broader impacts from our findings.